

Recognition of multi-carrier OFDM and single-carrier with alpha-stable distribution noise^①

He Jiai(何继爱)^②, Du Panpan^②, Wang Chanfei

(School of Computer and Communication, Lanzhou University of Technology, Lanzhou 730050, P. R. China)

Abstract

In order to identify the multi-carrier orthogonal frequency division multiplexing (OFDM) and the single-carrier signal in the non-Gaussian noise environment, different features of the two signals are analyzed in terms of five parameters: generalized normalized fourth-order cumulant, the maximum value of the instantaneous amplitude power spectral density, absolute standard deviation of instantaneous phase on the section with weak signals, and position and numbers of the generalized cyclic spectrum's peak. The recognition method of the multi-carrier OFDM and single-carrier signal is proposed in the environment with alpha-stable distribution noise. Simulation results show that the recognition rate of the multi-carrier OFDM can reach 100% when the mixed signal to noise ratio (MSNR) is greater than -5 dB and the recognition rate can reach 90% for the single-carrier when the MSNR is greater than 2 dB.

Key words: multi-carrier OFDM, feature parameters, modulation recognition, generalized cyclic spectrum, alpha-stable distribution

0 Introduction

With the rapid development of the communication system and Narrowband Internet of Things (NB-IoT)^[1,2], modulation recognition exhibits a diversified coexistence situation on multi-carrier and single-carrier in the communication signal modulation. Meanwhile, there are a number of non-Gaussian noise with spikes pulse and thick trailing in the received signals due to low-frequency atmospheric noise, multi-user interference and other effects^[3,4]. It is investigated that the noise can be considered as the noise with the alpha-stable distribution model effectively. In recent years, the intelligent radio technology has become the focus of attention in the communication systems, where modulation identification is an important part. Therefore, it is of great significance to study hybrid modulation recognition of multi-carrier and single-carrier in non-Gaussian environment.

There are two kinds of algorithms for identifying multi-carrier OFDM and the single-carrier signals. The first one is based on the wavelet transform domain, where the classification features are constructed to identify the OFDM and the single-carrier signals^[5-7].

The second is based on the high-order statistics. Akmouche proposed the algorithm to identify different signals by the fourth-order cumulant^[8]. After that, Li and Shi et al^[9,10] improved the algorithm. For the modulation recognition in the environment with alpha-stable distribution, signals with BPSK, QPSK, OQPSK, MSK and GMSK are identified with the fractal box dimension in Ref. [11]. The different signals are identified with the correlation coefficients of low-order cyclic spectral and generalized second-order cyclic statistics in Refs [12,13]. The signals modulated with 4ASK, BPSK, QPSK, 8PSK, MSK are identified by combining the generalized cumulant features with the generalized instantaneous phase features. However, the schemes mentioned above were investigated in the Gaussian environment. In addition, compared with traditional single-carrier signals, the multi-carrier is more difficult to extract, and the estimated parameters^[14,15] are more, which makes the research more complicated. Therefore, many related research results are still not completely enough, and they need further study. So it is motivated to investigate the recognition of the multi-carrier and the single-carrier signals in the non-Gaussian environment with alpha-stable distribution noise.

The rest of the paper is organized as follows. The

① Supported by the National Natural Science Foundation of China (No. 61561031, 61562058) and the Natural Science Foundation of Gansu Province (No. 1508RJZA054).

② To whom correspondence should be addressed. E-mail: 625620355@qq.com

Received on July 10, 2018

signal model with alpha-stable distribution is presented in Section 1. The characteristic parameters of the digital modulation signal is constructed in Section 2, where five feature identification parameters are given. In Section 3, the classifier is designed. Theoretical analysis and the simulation experiments are given in Section 4. Finally, the conclusion is derived in Section 5.

1 Signal model

In the noise environment with alpha-stable distributed, after the down-conversion processing, the baseband received signal can be expressed as

$$r(t) = s(t) + n(t) \quad (1)$$

where $s(t)$ is the baseband signal, $n(t)$ is the alpha-stable distribution noise. Five kinds of signals are considered in this paper, i. e. $s(t) \in \{s_{MASK}(t), s_{MPSK}(t), s_{MFSK}(t), s_{MQAM}(t), s_{OFDM}(t)\}$. The baseband signal of the multi-carrier OFDM is given by

$$S_{OFDM}(t) = \sqrt{\frac{E}{N_p}} \sum_k \sum_{n=0}^{N_p-1} C_{n,k} e^{j2\pi n \Delta f t} g(t - kT_s), \quad \Delta f = \frac{1}{N_p T_s} \quad (2)$$

where n is the subcarrier's index, $C_{n,k}$ is the transmitted data of the k -th subcarrier in the n -th symbol period, N_p is the number of subcarriers that are orthogonal to each other, T_s is the length of the OFDM symbol period. The baseband signals of the four kinds of single-carrier can be expressed as

$$S_{MASK}(t) = \sum_k a_k g(t - kT_s), \quad a_k \in \{(2k+1-M)d, k=0,1,\dots,M-1, d = \sqrt{3E/(M^2-1)}\} \quad (3)$$

$$S_{MFSK}(t) = \sqrt{E} \sum_k e^{j2\pi f_k t} g(t - kT_s), \quad f_k \in [k - \frac{M-1}{2}] \Delta f, k=0,1,\dots,M-1 \quad (4)$$

$$S_{MPSK}(t) = \sqrt{E} \sum_k e^{j\phi_k} g(t - kT_s), \quad \phi_k \in [\frac{2\pi}{M}k], \quad k=0,1,\dots,M-1 \quad (5)$$

$$S_{MQAM}(t) = \sum_k \sqrt{E_k} e^{j\phi_k} g(t - kT_s), \quad E_k = a_k^2 + b_k^2, \quad \phi_k = \tan^{-1}(b_k/a_k) \bmod 2\pi \quad (6)$$

where $g(t)$ is the shape pulse used by the baseband signal, T_s represents the symbol width, M is the modulation order, d represents 1/2 times of the distance between adjacent constellation points, E denotes the energy of the transmitted symbol, and Δf is the frequency interval, a_k and b_k in the MQAM signal are the signal's amplitude of the orthogonal carriers carrying the information. For the noise with alpha-stable distribution, it

is generally described by the characteristic function as Refs[16,17].

$$\varphi(t) = \exp\{j\mu t - \gamma |t|^\alpha [1 + j\beta \operatorname{sgn}(t)w(t, \alpha)]\} \quad (7)$$

$$w(t, \alpha) = \begin{cases} \tan(\pi\alpha/2), & \alpha \neq 1 \\ (2/\pi) \log |t|, & \alpha = 1 \end{cases} \quad (8)$$

where $\operatorname{sgn}(\cdot)$ is the sign function, $\alpha (0 < \alpha \leq 2)$ is the characteristic index which describes the degree of the distribution function's pulse, μ is the position parameter, $\gamma \geq 0$ is the dispersion coefficient which is similar to the variance under Gaussian distribution, $\beta (-1 \leq \beta \leq 1)$ is the symmetrical parameter. When $\beta = 0$, the stable distribution is symmetrical with u , which is called $S\alpha S$ for short. when $\mu = 0, \gamma = 1$, it is the standard alpha-stable distribution. In this paper, the standard alpha-stable distribution is used as the noisy model. For the noise with alpha-stable distribution, there does not exist statistics with the second-order and more than second-order. Thus, the mixed signal to noise ratio (MSNR), $Q_{MSNR} = 10 \lg(\sigma_s^2/\gamma)$ is exploited to describe the noise, where σ_s^2 indicates the signal variance, γ indicates the dispersion factor of alpha-stable distribution noise.

2 Derivation of the proposed algorithm

It can be proved that the OFDM signal obeys the asymptotic Gaussian distribution in the time domain by combining the central limit theorem with the characteristics of OFDM signal^[9]. Moreover, the more the number of the subcarriers, the stronger the Gaussian characteristics. The characteristics of approximating Gaussian are related to the number of subcarriers and it is nothing to do with the subcarrier modulation. In signal processing, for the signals or noise with Gaussian-distributed, their digital features and distribution functions can be represented with the first-order statistics (means) and the second-order statistics (variance or covariance). However, the first-order and second-order statistics can not be used for describing the signals or noises with non-Gaussian distribution. Thus, high order statistics are needed to extract the useful information of the signals. In this paper, the fourth-order cumulant features of the high-order statistics are exploited and a nonlinear function is designed, and then a generalized fourth-order cumulant is formulated to identify the multi-carrier and the single-carrier signal. The proposed algorithm is derived as follows. The modulus of the OFDM complex baseband signal model is given as

$$|S_{OFDM}(t)| = \sqrt{\frac{E}{N_p}} \sum_k \left| \sum_{n=0}^{N_p-1} C_{n,k} e^{j2\pi n \Delta f t} \right| \cdot g(t - kT_s) \quad (9)$$

The modulus of the fourth-order cumulant of the complex intermediate frequency (IF) signal is calculated as

$$\begin{aligned} cum_4(|S_{OFDM}(t)|) &= cum_4\left(\sqrt{\frac{E}{N_p}} \sum_k \left| \sum_{n=0}^{N_p-1} C_{n,k} \right| \cdot e^{j2\pi n \Delta f t} \cdot g(t - kT_s)\right) \\ &\quad (10) \end{aligned}$$

The Gaussianity of $\sum_k \left| \sum_{n=0}^{N_p-1} C_{n,k} \cdot e^{j2\pi n \Delta f t} \cdot g(t - kT_s) \right|$ is more than that of $\sum_k \sum_{n=0}^{N_p-1} |C_{n,k}| \cdot g(t - kT_s)$ | , therefore, the following is got:

$$\begin{aligned} &\sum_{n=0}^{N_p-1} C_{n,k} \cdot e^{j2\pi n \Delta f t} |, \text{ therefore, the following is got:} \\ &| cum_4(|S_{OFDM}(t)|) | \\ &= | cum_4\left(\sqrt{\frac{E}{N_p}} \sum_k \left| \sum_{n=0}^{N_p-1} C_{n,k} \cdot e^{j2\pi n \Delta f t} \cdot g(t - kT_s) \right| \right) | \\ &< | cum_4\left(\sqrt{\frac{E}{N_p}} \sum_k \sum_{n=0}^{N_p-1} |C_{n,k}| \cdot g(t - kT_s) \right) | \end{aligned} \quad (11)$$

The subcarrier modulation symbol and the modulation method are independent to each other. According to the semi-invariability of the cumulant, Eq. (11) can be written as

$$| cum_4(|S_{OFDM}(t)|) | < \left| \frac{1}{N_p^4} \cdot \sum_{n=0}^{N_p-1} cum_4\left(\sum_k |C_{n,k}| \right) \right| \quad (12)$$

For the subcarrier with MPSK and MFSK modulation, $|C_{n,k}|$ is a constant, the maximum of $| cum_4(\sum_k |C_{n,k}|) |$ is 2. For the subcarrier with the MQAM modulation, $|C_{n,k}|$ is contacted with M and $| cum_4(\sum_k |C_{n,k}|) | < 2$. Each subcarrier of OFDM is modulated by MPSK or MQAM. Hence, Eq. (12) can be rewritten as

$$\begin{aligned} &| cum_4(|S_{OFDM}(t)|) | \\ &\leq \left| \frac{1}{N_p^2} \cdot \sum_{n=0}^{N_p-1} cum_4\left(\sum_k |C_{n,k}| \right) \right| \\ &< \left| \frac{1}{N_p^2} \cdot \sum_{n=0}^{N_p-1} cum_4(1) \right| = \frac{2}{N_p} \end{aligned} \quad (13)$$

where $cum_4(1)$ is the cumulant of constant sequence 1 and $cum_4(1) = -2$. It can be seen that with the increase of the number of subcarriers, the fourth-order cumulant of the IF complex signal's modulus tends to be 0, and it is far less than that of the MPSK, MFSK and MQAM signals. Therefore, the multi-carrier OFDM and the single-carrier signals can be effectively identified by setting the appropriate decision threshold.

3 Construction of feature parameter

3.1 Features of generalized cumulant

In the environment with alpha-stable distribution, the amplitude of the signal changes due to introduction of a nonlinear function. However, the inequality between multi-carrier and single-carrier still exists. Based on this feature difference, the generalized fourth-order cumulant feature parameters C_{G42} are defined. Firstly, for the baseband signal in Eq. (1), two generalized second-order cumulant are defined as

$$C_{G20} = E[f(s(t))^2] \quad (14)$$

$$C_{G21} = E[|f(s(t))|^2] \quad (15)$$

where $E[\cdot]$ represents expectation, $f(\cdot)$ is the non-linear transformation given by

$$\begin{aligned} f(s(t)) &= \frac{\arctan |s(t)|}{|s(t)|} s(t) = \frac{\arctan |Ae^{j\phi}|}{|Ae^{j\phi}|} Ae^{j\phi} \\ &= \frac{\arctan |A|}{|A|} Ae^{j\phi} \\ &= \arctan |A| \cdot \text{sgn}(A) \cdot e^{j\phi} \end{aligned} \quad (16)$$

It can be seen from Eq. (16) that the non-linear transformation only maps the amplitude of the signals to a finite interval. It eliminates the large pulse of alpha noise, and does not change the phase information of the signals. Thus, the signals strayed by alpha-stable distribution noise have the second-order statistics or more. The generalized fourth-order cumulant is defined by

$$\begin{aligned} C_{G42} &= cum(f(s(t)), f(s(t)), (f(s(t)))^*, \\ &\quad (f(s(t)))^*) \end{aligned} \quad (17)$$

Assuming that $s(t)$ is the signal with zero mean and ergodic, then the generalized second-order and fourth-order cumulant can be estimated with the sampling data once as

$$\hat{C}_{G20} = \frac{1}{N} \sum_{n=1}^N f(s(n))^2 \quad (18)$$

$$\begin{aligned} \hat{C}_{G21} &= \frac{1}{N} \sum_{n=1}^N (f(s(n)), f(s(n))^*) \\ &= \frac{1}{N} \sum_{n=1}^N |f(s(n))|^2 \end{aligned} \quad (19)$$

$$\hat{C}_{G42} = \frac{1}{N} \sum_{n=1}^N |f(s(n))^4| - |\hat{C}_{G20}|^2 - 2\hat{C}_{G21}^2 \quad (20)$$

Without loss of generality, assume that the constellation's points have been normalized, i. e., $C_{G21} = 1$. The estimation of the normalized fourth-order cumulant is expressed as

$$G = \hat{C}_{G42} / \hat{C}_{G21}^2 \quad (21)$$

It can be shown from Fig. 1 that within the range of MSNR set, G of the OFDM signal is no less than

that of the single-carrier, such as MASK ($M = 2, 4$), BPSK, 4FSK and 16QAM. Starting from -5 dB, with the increase of MSNR, the difference is greater and greater. Thus, the multi-carrier OFDM can be distinguished from single-carrier signals effectively by setting a suitable threshold.

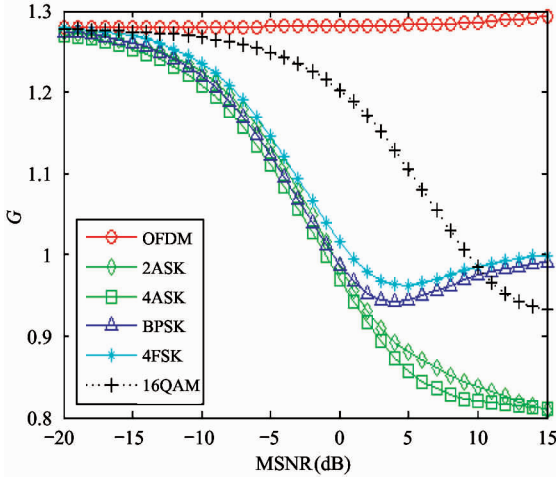


Fig. 1 The generalized normalized fourth-order cumulant G of signals changes with MSNR

3.2 Features of generalized instantaneous amplitude and phases

In the impulse noise environment, the received signal is $r(t)$, whose analytical signal is given by $z(t) = r(t) + jH[r(t)] = a(t)e^{j\varphi(t)}$, where $H[\cdot]$ is the Hilbert transform of the real signals, $a(t)$ is the generalized instantaneous amplitude of $z(t)$ expressed by

$$a(t) = \sqrt{r^2(t) + H^2[r(t)]} \quad (22)$$

The generalized instantaneous phase of $z(t)$ is written as

$$\varphi(t) = \arctan\left\{\frac{H[r(t)]}{r(t)}\right\} \quad (23)$$

As the existence of spectral aliasing in actual calculation, the modified sequence is defined as Ref. [18].

$$C(i) = \begin{cases} C(i-1) - 2\pi, & \varphi(i-1) - \varphi(i) > \pi \\ C(i-1) + 2\pi, & \varphi(i) - \varphi(i-1) > \pi \\ C(i-1), & \text{others} \end{cases} \quad (24)$$

The unfolded phase is

$$\varphi(i) = \varphi(i) - C(i) \quad (25)$$

Removing the components of the linear phase in Eq. (25), the true phase is obtained as

$$\varphi_{NL}(i) = \varphi(i) - \frac{2\pi f_c i}{f_s} \quad (26)$$

Thus, $\varphi_{NL}(i)$ is the generalized instantaneous

phase of $z(t)$. In order to extract the features conveniently, two characteristic parameters are determined as follows.

1) The maximum value of the spectral power density of the center normalization instantaneous amplitude r_{\max} expressed by

$$r_{\max} = \frac{\max\{FFT[a_{cn}(n)] \cdot \text{conj}\{FFT[a_{cn}(n)]\}\}}{N} \quad (27)$$

where N is the total number of sampling points, $a_{cn}(n)$ is the instantaneous amplitude given as $a_{cn}(n) = \frac{a(n)}{m_a}$

-1 , and $m_a = \sum_{i=1}^N \frac{a(i)}{N}$ is the average of instantaneous amplitude.

2) The standard deviation of the absolute value of the centered, non-linear component of the instantaneous phase expressed by

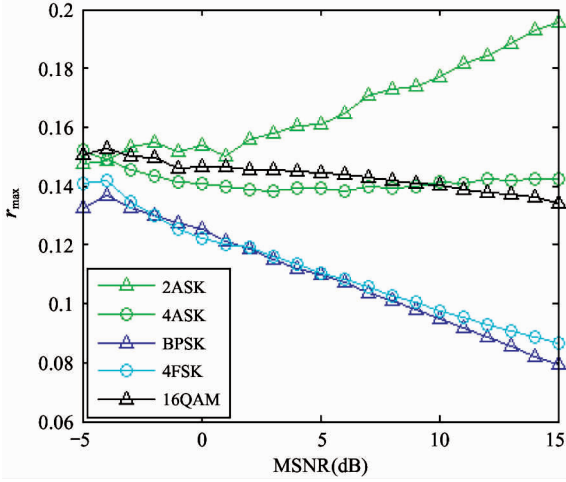
$$\sigma_{ap} = \sqrt{\frac{1}{C} \left(\sum_{a(n) > t_a} \varphi_{NL}^2(n) \right) - \frac{1}{C} \left(\sum_{a(n) > t_a} |\varphi_{NL}(n)| \right)} \quad (28)$$

where C is the number of instantaneous phase of the non-linear component, $a(n)$ is the instantaneous amplitude, t_a is the determined threshold of the non-linear signals and $\varphi_{NL}(n)$ is the non-linear instantaneous phase.

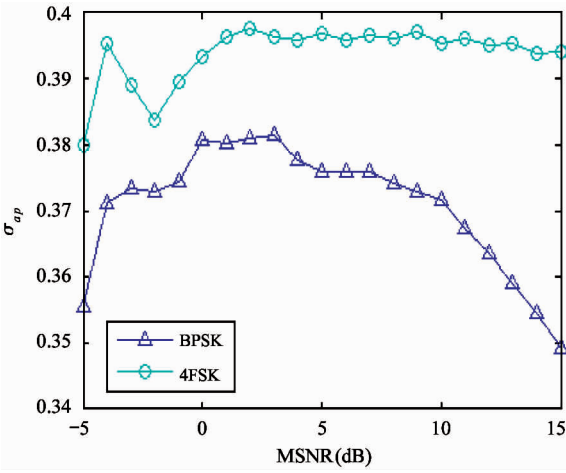
Simulations are presented to demonstrate the changing of parameter r_{\max} with MSNR. As shown in Fig. 2(a), the r_{\max} of 2ASK is always greater than 0.15 as $\text{MSNR} > 2\text{dB}$. r_{\max} of 4ASK and 16QAM signal is between 0.12 and 0.15. However, the amplitude of BPSK and 4FSK signal is no more than 0.12. According to the differences, the single-carrier modulation signals of 2ASK, 4ASK, BPSK, 4FSK, 16QAM can be divided into three categories. As shown in Fig. 2(b) that the phase of BPSK signal has two values and $\sigma_{ap} > 0.385$ when $\text{MSNR} > 0\text{dB}$. However, for the 4FSK, the non-linear instantaneous phase has four values and $\sigma_{ap} < 0.385$. According to the difference, the BPSK and 4FSK signals can be distinguished.

3.3 Features of generalized cyclic spectrum

As can be seen from Fig. 2(a), it is hard to distinguish the 4ASK and 16QAM with r_{\max} . However, it is analyzed that there are some differences on the cyclic spectrum. Two kinds of algorithms of the digital signal's spectrum correlation can be used^[19-21]: the Fourier transform and the time domain smoothing. In the paper, the latter is selected, and it can be employed as follows.



(a) The maximum of the spectral power density of the instantaneous amplitude r_{\max}



(b) The standard deviation of the absolute value of the non-linear component of the instantaneous phase σ_{ap}

Fig. 2 The features change with MSNR

1) Calculate N points spectrum of $r(n)$ at $T = NT_s$ as

$$R_T(k) = \sum_{n=0}^{N-1} r(n) \exp(-j2\pi nk/N) \quad (29)$$

2) Calculate the spectral correlation as

$$S_{rT}^\alpha(k) = \frac{1}{N} R_T(k + \alpha/2) R^*(k - \alpha/2) \quad (30)$$

3) Smooth the spectrum as

$$S_{rT}^\alpha(k)_{\Delta f} = \frac{1}{M+1} \sum_{m=-M/2}^{M/2} S_{rT}^\alpha(k+m) \quad (31)$$

N -point FFT can be equivalent to a bandpass filter whose bandwidth is $1/N$, and its center frequency is $f_k = k(f_s/N)$ and the output is the complex envelop of the signal. Therefore, the spectrum correlation analyzer can be replaced by N -point FFT for reducing the complexity. In the engineering, FAM algorithm is employed to smooth the time domain. The complexity is shown in Table 1.

Table 1 The complexity of the FAM algorithm

Calculation steps	Two complex signals' cycle cross spectrum complex multiplication times	Single signal's cycle spectrum complex multiplication times
N' -point FFT	$PN' \log_2 N'$	$P(N'/2) \log_2 N$
Frequency shift	$2N'P$	$N'P$
Multiply times	$(N')^2$	$P(N')/4$
FFT product sequence	$(N')/(P/2) \log_2 P$	$(N')^2/4[P/2] \log_2 P$

In Table 1, N is the sampling point's length in unit interval time. Defining M as the interval of the loop frequency's resolution and $N' = N/M$, $P = 4M$. Due to the parallelism of FAM algorithm, the operation time is reduced to $1/N'$ times of the original. The simulation results show that the proposed algorithm has good anti-noise performance, and thus, it provides a good theoretical basis for the system's implementation of modulation recognition under impulsive noise environment. The simulation results are shown in Fig. 3. Combined with the theoretical and simulation analysis, it is known that the 16QAM has peak as $\alpha = \pm \frac{m}{T_b}$ in the section of $f = 0$, and the peak's value arrives the maximum as $\alpha = 0$. However, the 4ASK has peak as $\alpha = 0, \alpha = \pm 2f_c \pm \frac{m}{T_b}$, and the maximum appears as $\alpha = \pm 2f_c$. Inspired by the difference, two characteristic parameters are defined as $T1$ and $T2$, where $T1$ stands for the position of the spectral peak, $T2$ stands for the number of the spectral peak. When $T1 = 0$ and $T2 > 3$, it indicates that the 16QAM signal can be recognized, otherwise the 4ASK signal.

4 Designing of the classification recognizer

The recognition algorithms are summarized as follows.

Step 1 Calculate parameter G based on the fourth-order cumulant to distinguish OFDM from the single-carrier MASK ($M = 2, 4$), BPSK, 4FSK, 16QAM.

Step 2 Calculate parameters r_{\max} and σ_{ap} based on the instantaneous characteristics. By using parameter r_{\max} to divide the single-carrier signals into three categories: 2ASK, 4ASK and 16QAM, BPSK and 4FSK. Then, 4FSK can be distinguished from BPSK with σ_{ap} .

Step 3 Calculate parameters $T1$ and $T2$ based on cycle spectrum. Then, 4ASK can be distinguished from 16QAM with the two parameters.

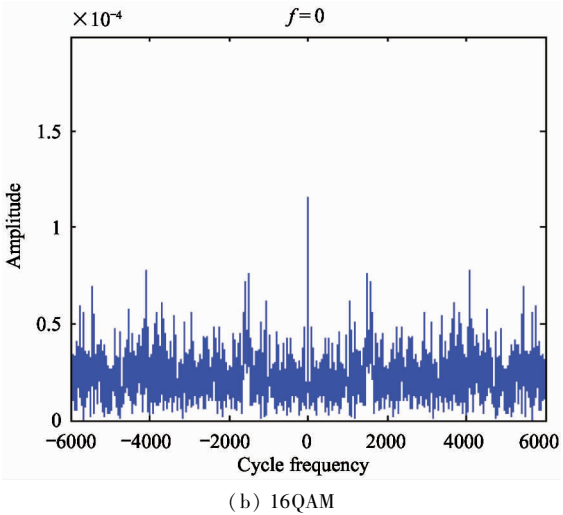
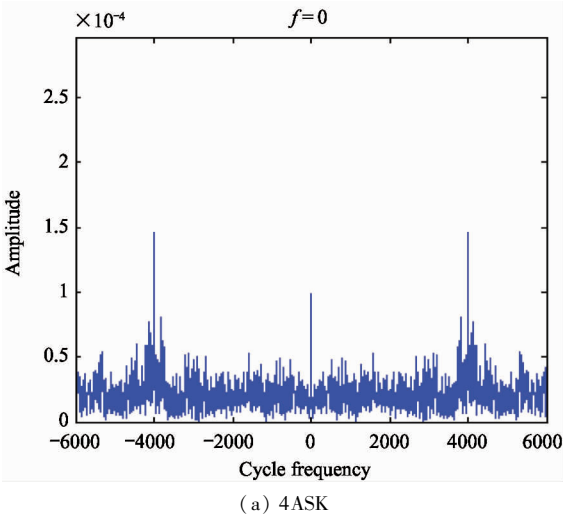


Fig. 3 Generalized cyclic spectrum of 4ASK and 16QAM signals

The flow diagram of the recognition algorithms is shown in Fig. 4.

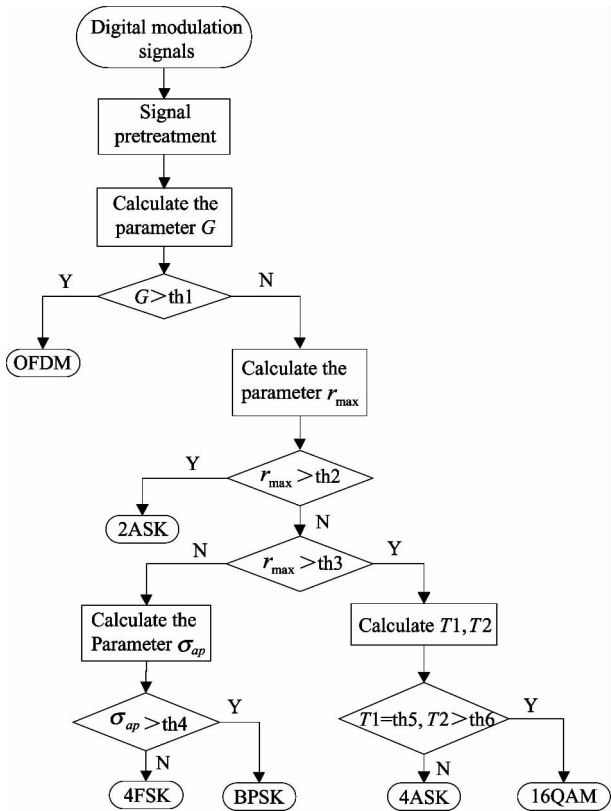


Fig. 4 Flow chart of decision making algorithm

5 Results and analysis

Simulations are presented to verify the validity of the proposed algorithm. The signal types and the specific parameters are given as Table 2 and the thresholds of each feature are shown in Table 3. The alpha-stable distribution noise is used. The symbol rate is 1 kB and

the sampling point is 1 024. The multi-carrier OFDM and the single-carrier signals are all normalized. In order to evaluate the performance of the algorithm, the correct recognition rate P is demonstrated as $P = (N_r/N) \times 100\%$, where N_r is the correct recognition times, N is the total number of experiments.

Table 2 Simulation on parameter setting	
Signal types	Values
OFDM	Numbers of subcarrier: 64, No protection interval, Modulation type of subcarrier: PSK, Baud rate: 1 000 baud/s, Carrier frequency: 3 kHz
ASK	2ASK/4ASK, Baud rate: 1 000 baud/s, Carrier frequency: 3 kHz
PSK	BPSK, Baud rate: 1 000 baud/s, Carrier frequency: 3 kHz
FSK	4FSK, Baud rate: 1 000 baud/s, Carrier frequency: 3 kHz
QAM	16QAM, Baud rate: 1 000 baud/s, Carrier frequency: 3 kHz

Table 3 Threshold of feature parameter					
th1	th2	th3	th4	th5	th6
1.28	0.15	0.12	0.385	0	3

1) Performance of recognition signals

The characteristic index of the alpha-stable distribution noise is 1.5, the MSNR changes from -20 dB to 15 dB. It can be seen from Fig.5 that the correct recognition rate of the signals raises with the increase of MSNR. For OFDM signal, the correct recognition rate reaches 100% as $\text{MSNR} = -5$ dB. For the single-carrier such as 4ASK, BPSK and 4FSK, the recognition

rate is up to 90% as $\text{MSNR} = -10$ dB. It demonstrates that the proposed algorithm can effectively recognize the multi-carrier OFDM and the single-carrier signals at low MSNR in the environment with alpha-stable distribution noise.

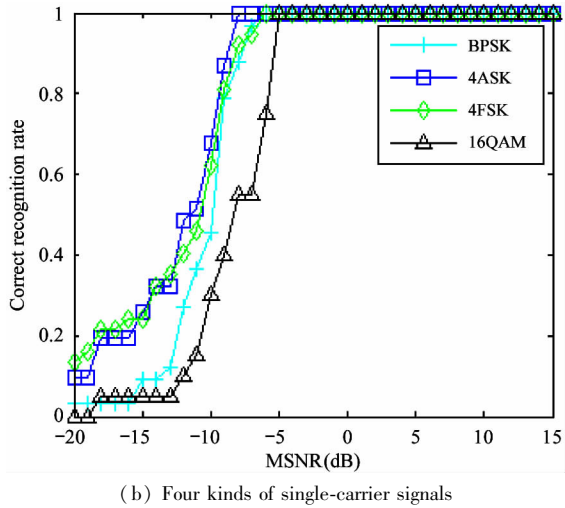
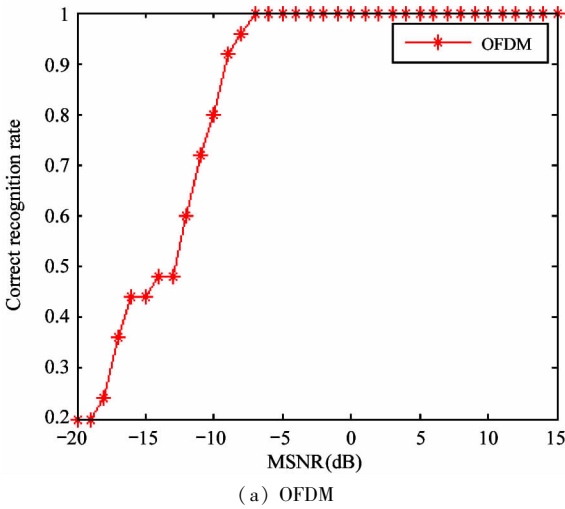


Fig. 5 The recognition rate of the signals with MSNR

2) Analysis of the factors affecting the recognition rate.

The characteristic index changes from 0.2 to 2 and MSNR is 0 dB. It can be observed from Fig. 6 that the recognition rate of the signals improves with the increase of α . For the OFDM signal, the recognition rate is up to 100% as $\alpha > 0.5$. For the single-carriers as 4ASK, BPSK, 4FSK, 16QAM, the recognition rate can reach 100% as $\alpha > 0.6$, and it is not affected by the characteristic index any more.

3) Recognition performance of the single-carrier signals with MSNR

It can be seen from Table 4 that the correct recognition rate of the signals as 2ASK, 4ASK, 16QAM can

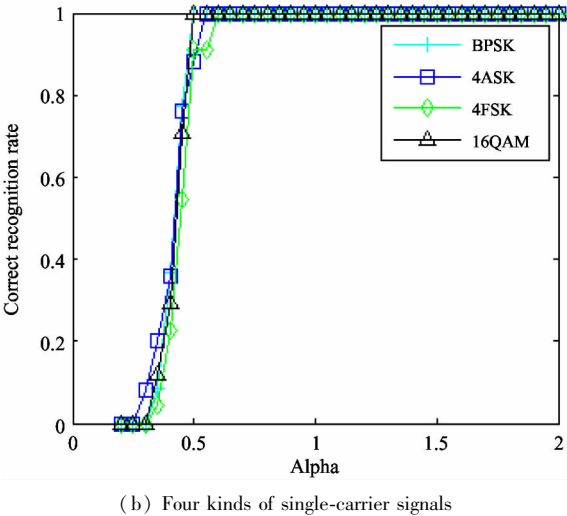
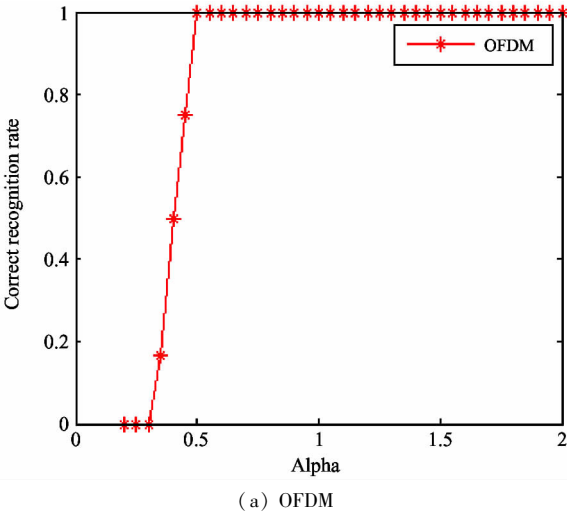


Fig. 6 The precognition rate of the signals with characteristic index

reach 100% as $\text{MSNR} > 0$ dB. For 4FSK signal, it is up to 100% as $\text{MSNR} > 2$ dB. For the signal with BPSK modulation, it is up to 97% as $\text{MSNR} = 5$ dB. Therefore, based on the features of the generalized instantaneous amplitude and phase and the generalized cyclic spectrum, a good performance can be achieved.

Signals	MSNR (dB)					
	-5	-2	0	2	5	10
2ASK	92.3	92.3	100	100	100	100
4ASK	0	50	100	100	100	100
BPSK	4.6	60.5	81.6	86.7	98.2	100
4FSK	0	75.5	82.4	100	100	98.9
QAM	0	0	100	100	100	100

4) Comparison of recognition algorithms
Based on the signals modulated with BPSK and

4FSK, the recognition rate of the proposed algorithm and that mentioned in Ref. [22] is compared when MSNR is 2 dB and 5 dB, and the comparison results are shown as Table 5. It can be seen that the recognition rate of the proposed algorithm is higher than that mentioned in Ref. [22] when MSNR = 2 dB. For the signal with 4FSK modulation, the recognition rate of the proposed algorithm reaches 100% when MSNR increases to 5 dB. Thus, the recognition rate of the proposed algorithm is higher than that mentioned in Ref. [22].

Table 5 Comparison of the proposed algorithm with that mentioned in Ref. [22]

Signal types	2 dB		5 dB	
	The proposed algorithm	Ref. [22]	The proposed algorithm	Ref. [22]
BPSK(%)	86.7	80	98.2	97.5
4FSK(%)	100	89	100	92.5

6 Conclusion

Modulation recognition of the multi-carrier and the single-carrier signals is proposed in the environment with alpha-stable distributed noise. Based on the generalized fourth-order cumulant, the generalized instantaneous amplitude and the generalized instantaneous phase feature in signal time domain, and the generalized cyclic spectrum feature in transform domain, five feature parameters are extracted to realize the modulation recognition of the multi-carrier OFDM and the single-carrier signals as MASK, BPSK, 4FSK and 16QAM. Simulations demonstrate that the proposed algorithm reduces the recognition complexity and the signal recognition rate. Moreover, the recognition rate of the proposed algorithm is still high when the characteristic index changes, which indicates that the proposed algorithm has good robustness. Therefore, it can be further used in the digital audio broadcasting and optical communication systems.

References

[1] Oh S M, Shin J S. An efficient small data transmission scheme in the 3gpp nb-iot system[J]. *IEEE Communications Letters*, 2017, 21(3): 660-663

[2] Wang Y P E, Lin X, Adhikary A, et al. A primer on 3gpp narrowband internet of things (nb-iot) [J]. *IEEE Communications Magazine*, 2016, 55(3):117-123

[3] Sokolov R I, Abdullin R R. Research of optimal pulse signal reception quality by mean risk minimum criterion with

action of Gaussian and non-Gaussian noise[C]. In: International Conference on Computational Techniques in Information and Communication Technologies, New Delhi, India, 2016. 97-100

[4] Feng P X, Wei P. Separation algorithm of independent component in multi-type noise[J]. *Journal of University Electronic Science and Technology*, 2017, 46(2): 352-356

[5] Giri R, Rao B D, Garudadri H. Reweighted algorithms for independent vector analysis[J]. *IEEE Signal Processing Letters*, 2017, 24(4): 362-366

[6] Walenczykowska M, Kawalec A. Type of modulation identification using wavelet transform and neural network [J]. *Bulletin of the Polish Academy of Sciences Technical Sciences*. 2016, 64(1): 257-261

[7] Tong C, Diao M, Yang C Z, et al. Multi-component signal modulation research based on joint independent component analysis and wavelet transform[J]. *Science Technology & Engineering*, 2016,16(30): 258-263

[8] Akmouche W. Detection of multicarrier modulations using 4th-order cumulant [C]. In: Military Communications Conference Proceedings, Atlantic City, USA, 1999. 432-436

[9] Li Y S, Luo M, Li X. The modulation recognition technology of OFDM signal based on higher order cumulant [J]. *Electronic Information Warfare Technology*, 2012, 27(4): 1-4

[10] Shi W J. Research and Implementation of Modulation Recognition Method of OFDM Signal [D]. Chengdu: Southwest Jiaotong University, 2015 (In Chinese)

[11] Liu G, Zhang J. Fractional lower order cyclic spectrum analysis of digital frequency shift keying signals under the alpha stable distribution noise[J]. *Chinese Journal of Radio Science*, 2017, 32(1): 65-72(In Chinese)

[12] Zhang Y D, Chen X Q, Zhan T M, et al. Fractal dimension estimation for developing pathological brain detection system based on minkowski-bouligand method[J]. *IEEE Access*, 2016, 4(99): 5937-5947

[13] Chavali V G, Silvac R C M. Detection of digital amplitude-phase modulated signals in symmetric alpha-stable noise[J]. *IEEE Transactions on Communications*. 2012, 60(11): 3365-3375

[14] Wang J, Yu H, Shu F, et al. Sum-MSE gain of DFT-based channel estimator over frequency-domain LS one in full-duplex OFDM systems [J]. *IEEE Systems Journal*, 2018: 1-10. Doi: 10.1109/JSYST.2018.2850934

[15] Shu F, Wang J, Li J, et al. Pilot optimization, channel estimation and optimal detection for full-duplex OFDM systems with IQ-imbalances [J]. *IEEE Transactions on Vehicular Technology*, 2017, 66(8): 6993-7009

[16] Ma H S. Parameter estimation and modulation identification of digital signals with alpha stable distribution noise [D]. Xi'an: Xidian University, 2013 (In Chinese)

- [17] Zhao C H, Yang W C, Ma S. Research on modulation recognition of communication signals based on generalized second-order cyclic statistics[J]. *Journal on Communications*, 2011, 32(1): 144-150
- [18] Wei Y J. Recognition of Modulation Pattern and Estimation of Parameter Based on Cyclic Spectrum[D]. Chengdu: University of Electronic Science and Technology of China, 2015 (In Chinese)
- [19] Yang J, Liu H, Bu X Y. Communication Signal Modulation Recognition: Principles and Algorithms[M]. Beijing: Post and Telecom Press, 2014. 5 (In Chinese)
- [20] Vučić D, Vukotić S, Erić M. Cyclic spectral analysis of OFDM/OQAM signals[J]. *AEUE-International Journal of Electronics and Communications*, 2017, 73:139-143
- [21] Tran T T, Nguyen D H N, Tuan D H, et al. Performance analysis of a spectrum sharing system in the modulation-based dimension [J]. *IEEE Transactions on Vehicular*

Technology, 2017, 66(12):10973-10988

- [22] Sun R F. Recognition of Digital Modulation Signals Based on High Order Cumulant and Spectral Analysis [D]. Hangzhou: Hangzhou Dianzi University, 2016 (In Chinese)

He Jiai, born in 1969, an associate professor. He is currently working at School of Computer and Communication of Lanzhou University of Technology. He received his B. S. degree from Northwest Normal University and M. S. degree from Lanzhou University in 1993 and 2004, respectively. His research interests include blind source signal separation, communication signal processing and parameter estimation, information control and multimedia coding and transmission.